INTERNATIONAL JOURNAL OF OPTIMIZATION IN CIVIL ENGINEERING
Int. J. Optim. Civil Eng., 2019; 9(3):373-393

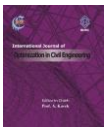

On Optimization of Resilient Rocking Cores

M. Grigorian[1*, †], A. Biglari[2], M. Kamizi[2] and E. Nikkhah[3]
[1]*MGA Engineering Inc, 111 N. Jackson St. Glendale, CA 91206, US*
[2]*Department of Civil Engineering, Faculty of Engineering, Golestan University, Gorgan, Iran*
[3]*University of Science and Culture, Tehran, Iran*

ABSTRACT

The research leading to this paper was prompted by the need to estimate strength and stiffness of Rigid Rocking Cores (RRCs) as essential elements of resilient earthquake resisting structures. While a limited number of such studies have been reported, no general study in terms of physical properties of RRCs, their appendages and adjoining structures have been published. Despite the growing knowledge on RRCs there are no design guidelines on their applications for seismic protection of buildings. The purpose of the present article is to propose effective rigidity limits beyond which it would be unproductive to use stiffer cores and to provide basic guidelines for the preliminary design of RRCs with a view to collapse prevention, re-centering and post-earthquake repairs/replacements. Several examples supported by computer analysis have been provided to demonstrate the applications and the validity of the proposed solutions.

Keywords: sustainability; rocking core; re-centering; collapse prevention; reparability; cost efficiency.

Received: 10 September 2018; Accepted: 8 February 2019

1. INTRODUCTION

Various applications of RRCs in combination with Earthquake Resisting Frames (RRCERFs) have been reported during the past fifteen years [1, 2 & 3]. The successful implementation of different types of RRCs for a number of significant projects have been published by [4, 5 & 6]. Summaries of beneficial attributes of RRCs as integral parts of earthquake resistant structures have been compiled amongst others by [7, 8 &9].

[*]Corresponding author: Senior Structural Engineering, MGA Structural Engineering Inc, 111 N. Jackson St. Glendale**,** CA 91206, US
[†]E-mail address: markarjan@aol.com (M. Grigorian)

Comprehensive accounts of rocking core innovations have been reported by [10 & 11]. The most recent development in this field is the use of RRCERFs in conjunction with replaceable energy dissipating links [12, 13]. Lately the concept has been extended to resilient earthquake resisting systems [14, 15]. The Seismic response of self-centering concentrically-braced frames as semi-rigid cores has been studied amongst others by [16,17,18,19&20]. One of the most recent earthquake resilient archetypes, proposed by the senior author, [13], Fig.1, is capable of damage control, elimination of residual stresses, Collapse Prevention (CP) and Post-earthquake Realignment and Repairs (PERR) [21, 22].

1.1 System description

The proposed system is both physically as well as conceptually different from its classical counterparts. The only physical difference between the proposed system and its conventional counterparts is in the purpose specific detailing that leads to resilient, highly reparable earthquake resisting structures that are both economical to build and inexpensive to repair.

Conceptually, performance levels are studied in terms of damage control and reparability, rather than expected damage at design level earthquakes. In fact, the proposed system advocates higher performance objectives than those stipulated in current codes of practice. The challenge here lays in the estimation of the minimum rigidity of the rocking core in such a way as to satisfy the expected resiliency conditions of the system. The proposed system [13, 23] is composed of commercially available building materials and components and consists of seven basic integral parts, i.e.

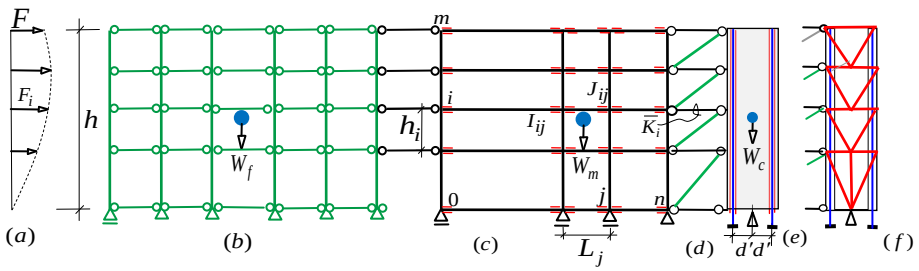

Figure 1. (a) Lateral loading, (b) Articulated gravity frame, (c) Moment frame + Energy dissipating connections, (d) Gap opening link beams and buckling restrained braces, (e) RRC+ stressed Tendons, (f) Braced frame RRC+ stressed Tendons

1) A physically articulated gravity system stabilized by adjoining Moment Frames (MF) and RRCs,
2) A steel or reinforced concrete (MF) with Grade Beam Restrained Column Supports (GBRCSs),
3) Beam end Replaceable Energy Dissipating Moment Connections (REDMCs) or similar devices;
4) A RRC, e.g., a pin supported steel braced frame, reinforced concrete or steel plated shear wall,
5) Vertical, unbonded stressed cables or Pre-compressed Springs (PCSs), as stabilizers of the RRC,
6) Axially rigid, pin ended, horizontal Link Beams (LBs) or functionally similar devices,

7) Especially designed and detailed RRC-Diaphragm interfaces.

Several sets of supplementary devices can be integrated as part of the proposed system, e.g.

1) Modified post-tensioned Gap Opening Link Beams (GOLBs) or functionally similar devices,
2) Buckling Restrained Columns (BRBs) or similar elements placed between the MF and the RRC
3) Any set of energy absorbing devices that may be deemed suitable for the project, e.g. Slotted–bolted friction connections [24], Viscoelastic dampers [25], etc.,

The most remarkable attribute of the RRC is its ability to force the companion Earthquake Resisting Frame (ERF) and energy dissipating devices to act as members of Structures of uniform Response (SUR), (Appendix B). SUR are weight optimized lateral resisting systems in which story level drift ratios are constant and members of similar groups such as beams, columns, braces, connections and structural appendages share the same demand-capacity ratios regardless of their location within the system [26, 27]. Since groups of members of SUR can be identical then they would be more efficient to build and repair than their conventional counterparts.

However, in order to design efficient RRCERF combinations, it is necessary to first develop realistic RRCs that are practical in size and can function as efficiently as infinitely rigid cores. Similarly, the core and the designated appendages should be able to realign the ERF and the adjoining gravity system after a given seismic event. The general functions of common types of RRCs and their appendages are briefly discussed in the next section.

While commercially available software can be used to analyze and design most complicated RRC related systems, the following manual methods of analysis may also be considered for assessment of the relative rigidities of practical rocking cores.

1) Drift control methodologies [28],
2) Quasi-static analysis of rocking wall systems [29],
3) Maximum core displacements [3], (Appendix A), and
4) The frequency equivalency method introduced in section 6 of the current contribution.

The present article introduces two competing criteria for the preliminary assessment of minimum rigidities above which SDOF behavior can be assured for solid rocking cores, i.e., the frequency related concept, section 6 below, and the minimum displacement criterion, presented under sections 2.1. The remainder of this paper is concerned with establishing a simple technique for practical design of solid RRCs with collapse prevention and re-centering capabilities. This is achieved by selecting a simple theoretical model that lends itself well to manual computations, reflects the true behavior of the prototype without loss of accuracy and helps establish physical limits beyond which neither the drift differential nor higher frequencies of the RRC can influence the response of the combined system.

2. RRC RESPONSE AND FUNCTION

Four generic RRCs constructed out of stiffened plywood, steel plated shear walls, reinforced concrete and steel braced frames are shown in Figs. 2(a), (b) (c) and (d) respectively. The

main function of the RRC and the stabilizing devices is to reduce seismic demand on ERFs, impose uniform drift, prevent soft story failure, suppress higher modes of vibrations, provide support for supplementary elements, and help implement the PERR process. It has been shown [30] that in contrast to RRCs, higher modes of vibrations can have structurally adverse effects on fixed base, non-rigid shear walls, after formation of plastic hinges at the supports.

The high rigidity of the core causes its own as well as all components of the ERF and supplementary devices to undergo equal rotations and to absorb proportional amounts of energy. The entire structure including the relatively softer ERF/MF acts as a SDOF system and allows the rigid core to tilt as a statically determinate upright beam. This forces the reference line of displacements to pass through both the pin and the free end of the RRC. It also forces all points of contra flexure to occur at mid-spans and mid-heights of beams and columns respectively. In addition, the RRC tends to redistribute the seismic and P-delta moments and shears rather evenly between groups of similar members such as beams, columns and braces of equal lengths and heights respectively. This is due to the fact that in RRCERFs the shear in the frame tends to be uniform over the height of the ERF [31].

The physical behavior of the RRCERF can best be visualized by the ERF and the RRC resisting the lateral forces together until the frame becomes a stable mechanism. Seismic shears are transferred to the RRC through LBs, PCSs, BRBs as well as specially detailed connections between the slab and the core, such as that shown in Figs. 3 (a) and (b) that allow transmission of seismic shears from the diaphragm to the RRC without damaging the floor-core interface, [17, 32, 33]. Fig. 3 (a) also shows that the location of the center of most critical hole at the left-hand end of the connecting angle with respect to center of rotation of the RRC can be defined by radius r and radial inclination θ.

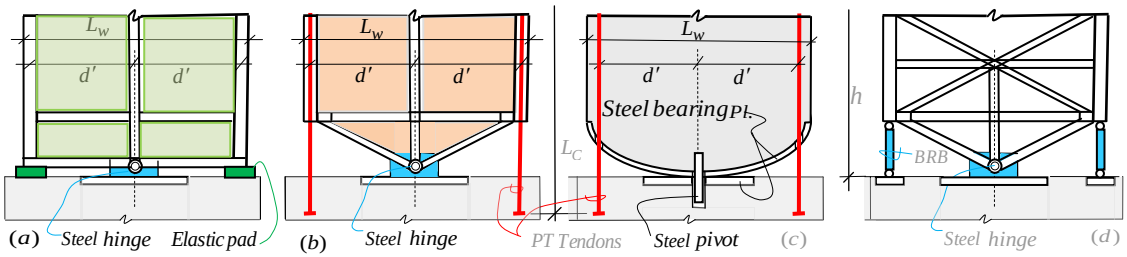

Figure 2. (a) Plywood RRC, (b) Steel plated RRC, (c) Reinforce concrete RRC, (d) Braced frame RRC+BRBs

An un-stabilized RRC is neither capable of preventing collapse nor re-centering the system. The restoring capabilities of free standing RRCs are defined by their ultimate strength and base level rotational stiffness. An expanded list of attributes of well-designed RRCs is presented in section 7 and Appendix B.

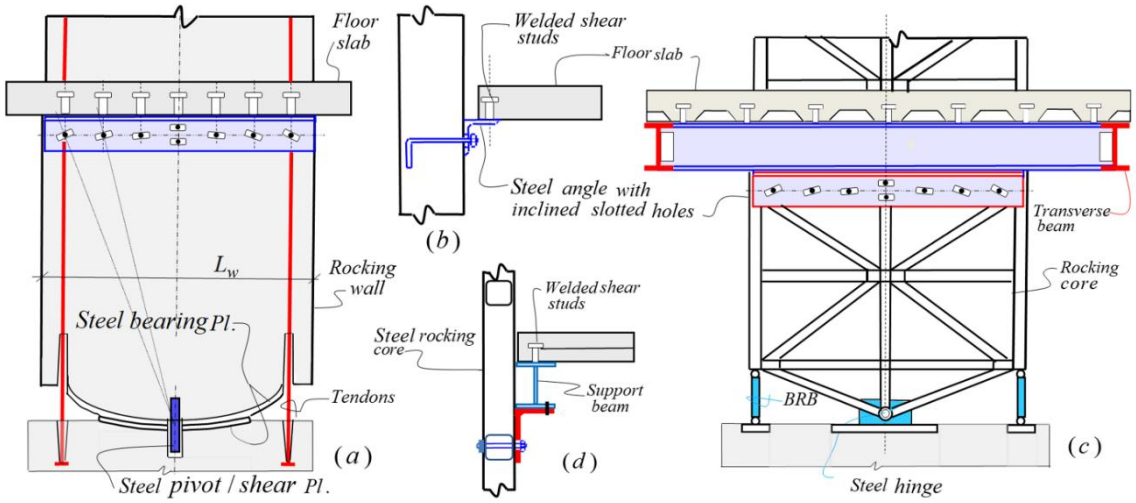

Figure 3. (a) Concrete RRC & diaphragm connection, (b) Side view of (a), (c) BRB enhanced Steel RRC and diaphragm connection, (d) Side view of (c)

2.1 Core stiffness

Experience has shown that a free standing rocking core or stiff spine may be considered as sufficiently rigid if its maximum drift differential under lateral forces does not exceed more than ten percent of the uniform drift of the ERF, i.e. $\phi_{Core} \le 0.10\phi_{unif}$ [3], Fig. 4 shows the results of one such study where the normalized variations, ϕ / ϕ_{unif} of the proposed structural system is plotted against the variations of the relative rigidities of the ERF and the core $[K_{frame} / K_{core}] \approx [\text{Constant}/t_{core}]$, where t_{core} is the thickness of a prismatic core. The solid and dashed lines correspond to first floor and roof level drift variations respectively. It may be noted that both the roof and first floor level drift differentials are zero at $t_{core} = \infty$ and diverge to 5% and 9% at $t_{core} = 1$ in (25.4 mm) and $t_{core} = 2$ in (50.8 mm) respectively. This implies that for all practical intents and purposes the rigidity of the core can be based on $\phi_{Core} \le 0.10\phi_{unif}$ or smaller as the case may require.

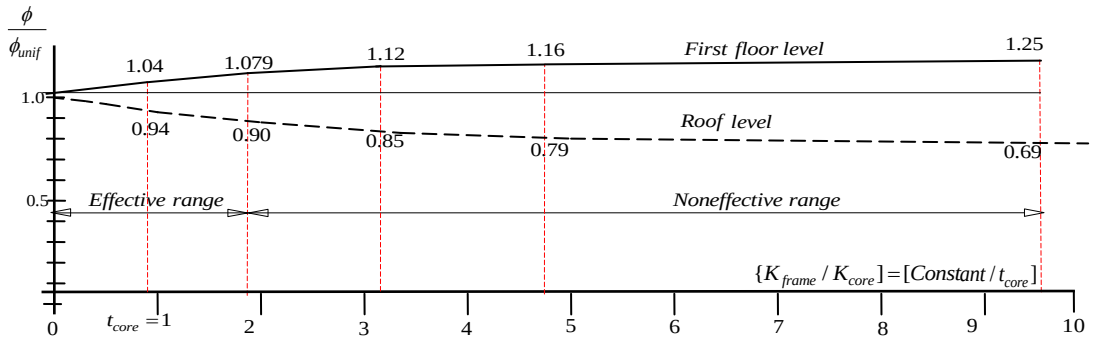

Figure 4. Effect of rocking core rigidity on the uniform drift ratio

2.2 Core base spring stiffness

The strength and stiffness of the RRC and its appendages are the two most important factors that help sustain the integrity of the damaged structure during the PERR process. The main function of the unbonded tendons, PCSs/BRBs, energy absorbing pads and similar devices is to stabilize the RRC, prevent collapse, to realign the system and to help implement the PERR process. These devices and the pivot at the base constitute energy absorbing springs that are expected to exhibit elastic-plastic response during and after seismic events. The limited purpose of this section is to establish a relationship for the interacting force of the uppermost link beam in terms of the rigidities of the MF and the rocking core. The stress-strain relationship of the wall base spring can be expressed as $\phi = M_S / k_S$, where M_S and k_S are the moment of resistance and the rotational stiffness of the spring respectively. Strain compatibility between tendon stretching and spring rotation before decompression requires that $\phi d' = \pm\varepsilon$. Substituting for $\varepsilon = T_t h / A_t E_t$ and $M_S = 2T_t d'$ in the strain equation gives, $k_s = 2d'^2 A_t E_t / h$. Subscript *t* refers to core total tendon force, $T_t = T_0 \pm M_S / 2d'$, and the initial tension T_0 should be large enough to realign the collapsing MF to its original position. In order to appreciate the contribution of the RRC in the absence of other auxiliary devices, consider the static interaction of the MF and the RRC as illustrated in Figs. 5(c), (d) and (e).

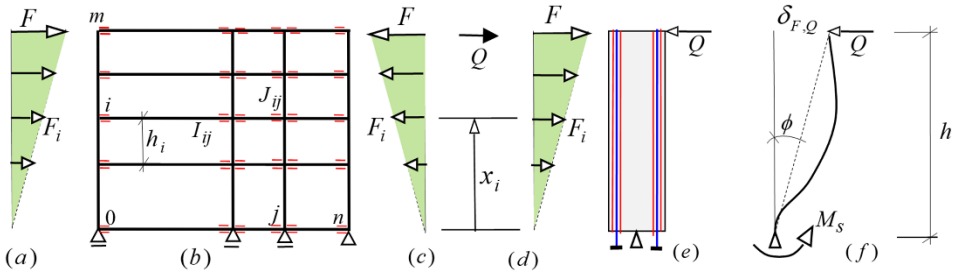

Figure 5. (a) Loading, (b) MF (c) Reactive forces on MF, (d) Reactive forces on RRC, (e) RRC, (f) Drift profile

2.2.1 Seismic load distribution

Results presented in this work are sensitive to seismic load distribution. However, if the core is sufficiently rigid the seismic load distribution will closely resemble the triangular profile recommended by most codes of practice [20], Fig. 5 (a). If the MF is regular i.e. $h_i = \bar{h}$ then the magnitude of the story level lateral forces can be estimated as $F_i = Fx_i / m$, whence the maximum tip displacement and base moment of the spring supported flexible cantilever of Fig. 5 (f) can be expressed as;

$$\delta_{C,F.} = \frac{F\bar{h}^3}{360EI}(33m^4 + 60m^3 + 25m^2 + 2) + \frac{M_0(m)}{k_s} = \frac{F\bar{h}^3 f(m)}{360D_C} + \frac{M_0(m)}{k_s} \quad (1)$$

$$M_0(m) = (m+1)(2m+1)\frac{F\bar{h}}{6}, \tag{2}$$

Respectively, where *m* is the number of stories of the MF. Furthermore, the core will tend to resist the entire seismic load by itself [9], as shown in Figs. 5 (d) and (e), where *Q* is the reactive force acting on top of the core. Whether the core is modeled as an upright simply supported beam or a propped cantilever with a spring, as in Fig. 5 (f), the static equilibrium of the core requires that; $Qh + M_S = M_0(m)$. Next, if $\delta_{F,Q}$ is the maximum displacements of the MF due to *Q* and $\delta_{C,Q}.\delta_{C,F}$, $\delta_{S,Q}$ and $\delta_{S,F}$ are the corresponding displacements of the RRC due *Q*, F_i and the M_S respectively, then displacement compatibility can be achieved if $\delta_{F,Q} = \delta_{S,F_m} + \delta_{C,F_m} - \delta_{C,Q} - \delta_{S,Q}$, i.e.

$$\frac{Qm^3\bar{h}^3(1+\rho)}{24D_F} = \frac{M_0(m)\bar{h}}{k_s} + \frac{Fm^3\bar{h}^3 f(m)}{360D_C} - \frac{Qm^3\bar{h}^3}{3D_C} - \frac{Qm^2\bar{h}^2}{k_s} \tag{3}$$

where, $D_F = E_f J$, $J = (h/2)\sum_{i=1}^{m}\sum_{j=0}^{n}(J_{i,j}/h_i)$ per Eq. (14), $D_C = E_c I_c$ and $\rho = JL/Ih$. Subscripts *F* and *C* refer to the MF and core respectively. Eqs.1, 3 and 4 are ideally suited for the practical design as well as comparative studies of RRC/MF combinations with different numbers of stories. However, for the purposes of the current study the seismic profile has been assumed to be a continuous function of the variable *I* regardless of number of stories *m*. Eq. (3) can be simplified greatly by replacing the discretized loading profile with its equivalent continuous counterpart, i.e.,

$$\frac{Qh^3(1+\rho)}{24D_F} = \frac{2\bar{F}h^2}{3k_s} + \frac{11\bar{F}h^3}{60D_C} - \frac{Qh^3}{3D_C} - \frac{Qh^2}{k_s} \tag{4}$$

Here $\bar{F} = Fh/2$ is the total seismic shear force. Substituting for $K_S = k_s/h^2$ $K_F = 24D_F/(1+\rho)h^3$, $K_C = 3D_C/h^3$ and $\bar{K}_C = 60D_C/11h^3 = 20K_C/11$, then Eq. (4) can be rewritten as;

$$\frac{Q}{K_F} = \frac{2\bar{F}}{3K_s} + \frac{\bar{F}}{\bar{K}_C} - \frac{Q}{K_C} - \frac{Q}{K_s} = \left[\frac{2}{3K_S} + \frac{11}{20K_C}\right]\bar{F} - \left[\frac{1}{K_S} + \frac{1}{K_C}\right]Q \tag{5}$$

These leads, after rearrangement to determination of the roof level interacting force;

$$\frac{Q}{\bar{F}} = \left[\frac{2}{3K_s} + \frac{11}{20K_C}\right] \Big/ \left[\frac{1}{K_F} + \frac{1}{K_S} + \frac{1}{K_C}\right] \tag{6}$$

Note that as $K_S \to 0$, the interactive force becomes $Q = 2F/3$. Once load Q is known the flexural deformations of the core acting as a tilted simply supported beam can be estimated as;

$$\delta_{core} = \frac{Fh^4}{360E_cI_c}\left[7(\frac{x}{h}) - 10(\frac{x}{h})^3 + 3(\frac{x}{h})^5\right] + \frac{(2F-3Q)h^3}{18E_cI_c}\left[3(\frac{x}{h})^2 - (\frac{x}{h})^3 - 2(\frac{x}{h})\right]\frac{1}{2} \tag{7}$$

and

$$\theta_{core} = \frac{Fh^3}{360E_cI_c}\left[7 - 30(\frac{x}{h})^2 + 15(\frac{x}{h})^4\right] + \frac{(2F-3Q)h^2}{18E_cI_c}\left[6(\frac{x}{h}) - 3(\frac{x}{h})^2 - 2(\frac{1}{h})\right] \tag{8}$$

Alternatively, if $\bar{M}_S$ is the spring moment due to bending of the core, and $\theta_{C,F}, \theta_{C,\bar{M}}$, and $\theta_{S,\bar{M}}$ are defined as the lower end rotations of the core and spring acting as a simply supported beam, due to F and $\bar{M}_S$ respectively, then rotational compatibility, $\theta_{C,F} - \theta_{C,\bar{M}} = \theta_{S,\bar{M}}$, gives;

$$\frac{7Fh^3}{360E_cI_c} - \frac{\bar{M}_S h}{3E_cI_c} = \frac{\bar{M}_S}{k_s} \text{ or } \bar{M}_S = \frac{Fh^2}{120\left[1 + \frac{3D_C}{k_S h}\right]} \tag{9}$$

It follows that δ_F and δ_C corresponding to roof level and core maximum displacements at *x=0.5193h* respectively can be estimated as;

$$\delta_F = \frac{Q}{K_F} \text{ and } \delta_C = \frac{\delta_F}{1.926} + \frac{0.0652Fh^4}{D_C} - \frac{0.0616\bar{M}h^2}{D_C} \tag{10}$$

3. STATICS & MODEL TRANSFORMATION

The purpose of this section is not to present an expose on the mathematical treatment of the proposed structure, but rather to take advantage of its abilities to present itself as a SDOF system. The knowledge that the combined structure is forced to tilt through a rigid body rotation ϕ, Fig. 5 (f), helps reduce the task of otherwise cumbersome analysis to manually manageable solutions. Therefore;

$$\delta_F = \frac{V_f}{K^*} = \frac{V_f h}{hK^*} = \frac{M_0}{hK_F^*} = \frac{M_0}{hK_F} \text{ and } M_0 = \sum_{i=1}^{m} F_i x_i = V_f h, \tag{11}$$

M_0 is the total external moment acting on both the prototype, Fig. 6 (a), and the equivalent model Fig. 6 (b). Eq. 11 can be rewritten in terms of drift ϕ, which is constant along the heights of both the model and the prototype.

$$\phi = \frac{\delta}{h} = \frac{V_f}{hK^*} = \frac{V_f h}{h^2 K^*} = \frac{M_0}{h^2 K_F^*} = \frac{M_0}{h^2 K_F} \tag{12}$$

K_F^* and $K_F^* = K_F$ are the global angular stiffnesses of the prototype and the equivalent MF respectively, i.e.

$$\phi_F = \frac{M_0}{12E}\left[\frac{1}{\sum_{j=0}^{n}\sum_{i=1}^{m}(J_{i,j}/h_i)} + \frac{1}{\sum_{j=1}^{n}\sum_{i=0}^{m}(I_{i,j}/l_j)}\right] = \frac{M_0}{h^2 K_F^*} \tag{13}$$

The transformation to the single module formulation directly derived from Eq. (13) results in;

$$\phi_F = \frac{V_f h^2}{12E}\left[\frac{h}{2J} + \frac{L}{2I}\right] = \frac{M_0}{h^2 K_F}, \; 2(I/L) = \sum_{i=0}^{m}\sum_{j=1}^{n}(I_{i,j}/l_J) \text{ and } 2 \\ (J/h) = \sum_{i=1}^{m}\sum_{j=0}^{n}(J_{i,j}/h_i) \tag{14}$$

Eq. (14) describes completely the elastic response of the prototype under lateral forces 1(a). A brief verification of Eq. (14) can be found in [17, 34]. Since the total gravity force on both models is $P = W_F = W_f + W_c$, then the total external moments in terms of the *P*-delta effect can be expressed as $(M_0 + M_{P\Delta})$, where $M_{P\Delta} = P\phi h$. Considering the use of the notional shear force $\bar{V}$ which acts in the same location and sense as V_f and results from the notional equilibrium equation $P\delta = P\phi h = \bar{V}h$, Eq. (2) can be replaced with;

$$\phi = \frac{M_0}{h^2 K_F^* - Ph} \text{ and } \phi = \frac{M_0}{h^2 K_F - Ph} \tag{15}$$

It follows therefore that $P = hK_F$ can be regarded the critical gravity load of both models.

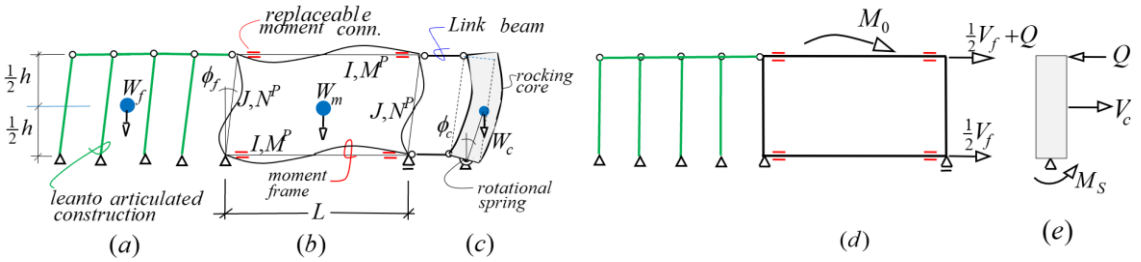

Figure 6. (a) articulated gravity system, (b) Grade beam supported MF, (c) Rigid rocking core, (d & e), Free body diagrams

3.1 Plastic analysis

Seismic response is associated with ultimate loading conditions, and as such maximum carrying capacity of any structure at incipient collapse should be carefully studied [35, 36]. The rocking ability of the wall improves the distribution of displacements but not the maximum drift at roof level, and it does not always improve the ultimate carrying capacity of the MRF. While it is known that wall-mounted and/or base-level energy-dissipating devices can improve both the ultimate capacity and the drift development characteristics of the combined structure, it is deemed rational to ignore the contributions of such devices in favor of higher load factors at incipient collapse. The use of MFs in conjunction with RRCs leads to preferred plastic collapse mechanisms as shown in Figs. 7(b) and (d). Obviously, if the core is to prevent soft story failure then it should be capable of imposing a sway type mechanism upon the ERF without developing plastic hinges along its height, i.e. $M^P_{Core} > M^P_F$. The virtual work equations for the two un-supplemented models can be expressed as;

$$\text{For the prototype } (M_0^P + M_{P\Delta})\theta = \sum_{i=1}^{m} F_i x_i \theta = \sum_{i=0}^{m}\sum_{j=1}^{n} 2M^P_{i,j}\theta \tag{16}$$

$$\text{For the equivalent model } (M_0^P + M_{P\Delta})\theta = \sum_{i=1}^{m} F_i x_i \theta = 4M^P\theta \tag{17}$$

θ is a small virtual rotation. It has been observed that regular MFs combined with RRCs adapt a unique mode of response where all elements undergo the same rotation and drift ratios respectively. Therefore, the prototype, Fig. 7(a), can also be modeled as the transformed option for plastic design purposes. The plastic moment of resistance, M^P_F of both models with no supplementary devices, can be assessed as;

$$(M_0^P + M_{P\Delta}) = M^P_F = \sum_{i=0}^{m}\sum_{j=1}^{n} 2M^P_{i,j} = Qh = 4M^P_{transferred} \tag{18}$$

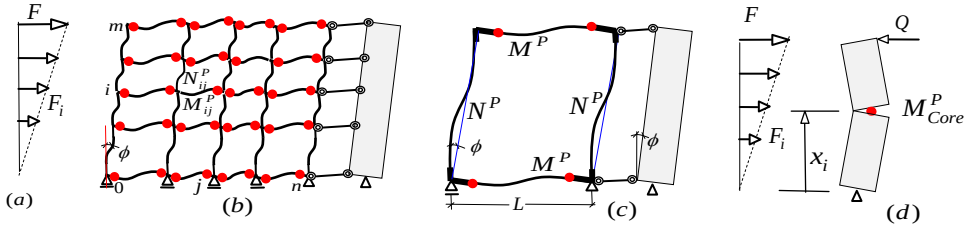

Figure 7. (a) Loading, (b) Prototype and preferred failure pattern, (c) Single bay equivalent model, (d) RRC failure mode

As, F_i is directly transferred to the rigid core as depicted in Fig. 7(d), then the plastic moment of resistance of the core can be estimated as;

$$M_{Core}^{P} = \frac{Pax}{6m}(m^2 - x^2 - x + 1) \tag{19}$$

where x is the nearest integer to $x = \left[-1 + \sqrt{1 + 4(m^2 - 1)/3}\right]/2$. Eqs (15,18&19) make the proposed configuration amenable to ASD, LRFD, Plastic and Performance based design treatments. Obviously the RRC should also be designed for maximum horizontal shear *Q* near the upper support. For a rigorous proof of the mathematical transformations (14) and (18) the reader is referred to [17], where transformation models for LBs and BRBs are also discussed.

4. ANALYSES OF FLEXIBLE ROCKING CORES

An understanding of the influence of flexible cores on global response of RRCERFs is a priori to establishing similar arguments for the effects of RRCs on companion structures. The frame and the core masses can be defined as $m_F = m_f + m_m$ and m_C respectively. Since forces $W_F = W_f + W_m$ and W_m act at mid height of the module only $W_F/2$ of the envisaged shear force would act at height *h*, Fig. 5(a). However since $(V_F/V_C) = (W_F/W_C) = (m_F/m_C) = \alpha_m$, then the free body diagrams of Figs. 5 (d, e), in the absence of the *P*-delta moment, would lead to the equilibrium equation; $M_0 = -M_S + (V_f + V_c)h/2$, where M_S is the moment of resistance of the core base rotational spring. Since the core and the MF are in static equilibrium then the following equation of compatibility for roof level displacements can be written down in terms of V_f, V_c and the interacting force *Q*, as;

$$\frac{(V_f + Q)h^3(1+\rho)}{24D} = \frac{5V_c h^3}{48D_C} + \frac{V_c h^2}{2k_S} - \frac{Qh^3}{3D_C} - \frac{Qh^2}{k_S} \tag{20}$$

$D_F = E_f J_f$, $D_C = E_c I_c$ and $\rho = JL/Ih$. Subscripts f and c refer to the MF and core respectively. If $K_F = 24D_F/(1+\rho)h^3$, $K_C = 3D_C/h^3$, $\overline{K}_C = 48D_C/5h^3$ and $K_S = k_s/h^2$, then Eq. (20) reduces to;

$$\frac{(V_f + Q)}{K_F} = \frac{V_c}{\overline{K}_C} + \frac{V_c}{2K_S} - \frac{Q}{K_C} - \frac{Q}{K_S} \tag{21}$$

which leads, after rearrangement, to determination of the link/interacting force;

$$Q = \frac{\left[\frac{V_c}{2K_S} + \frac{V_c}{\overline{K}_C}\right] - \left[\frac{V_f}{K_F}\right]}{\left[\frac{1}{K_F} + \frac{1}{K_S} + \frac{1}{K_C}\right]} \tag{22}$$

Note that as $K_S \to 0$, the interactive force becomes $Q = V_c/2$. Once Q is known, δ_F and δ_C corresponding to roof level and core mid-height displacements respectively can be estimated as;

$$\delta_F = \frac{V_f + Q}{K_F} \text{ and } \delta_C = \frac{\delta_F}{2} + \frac{V_c h^3}{48D_C} - \frac{(V_c - 2Q)h^3}{32D_C} \tag{23}$$

Defining the net drift of the center of mass of the core with respect to its nearest support it gives;

$$\phi_{c,net} = \frac{\delta_C}{h} - \frac{\delta_F}{2h} = \frac{V_c h^2}{48D_C} - \frac{(V_c - 2Q)h^2}{32D_C} \tag{24}$$

If $D_C \to \infty$ and $M_0 \to (M_0 + M_{P\Delta})$, then $V_f \to V_f + P\delta_F/h$, subsequently Eqs. (23) and (24) yield;

$$Q = V_c/2 - K_S\delta_F,\ \delta_F = h\phi = \frac{(V_f + V_c/2)h}{[h(K_F + K_S) - P]} \text{ and } \delta_C = \frac{\delta_F}{2} \tag{25}$$

The following examples have been devised to demonstrate the applications of the formulations presented under sections 3 and 4 above.

Example 1: Relatively flexible rocking core-determination of δ_F, δ_C and ω.

Let E=29000ksi, h=L=10.0ft. $I_f = J_f = 1142025$ in^4 $I_c = 124242$ in^4, $W_f = 5000$ kips,

$W_c = 500$ kips, $k_s = 5000$ kip-ft. /rad and $\rho = 1.0$.

Solution: $\alpha_m = \dfrac{5000}{500} = 10,$

$$\frac{1}{K_F} = \frac{1728 \times 1000}{12 \times 29000 \times 11420.25} = 0.000435,$$

$$\frac{1}{2K_S} = \frac{144 \times 100}{2 \times 5000 \times 12} = 0.12, \qquad \frac{1}{K_C} = \frac{1728 \times 1000}{3 \times 29000 \times 1242.42} = 0.01599,$$

$$\frac{1}{\bar{K}_C} = \frac{5 \times 1728 \times 1000}{48 \times 29000 \times 124242} = 0.00499, \qquad \frac{1}{K_S} = \frac{144 \times 100}{5000 \times 12} = 0.24,$$

Eq. (22) gives; $Q = \dfrac{500(0.00499 + 0.12000) - 2500 \times 0.000434}{0.24543} = 239.42$ kips [239.4 kips]

Eq. (23) gives; $\delta_F = \dfrac{V_f + Q}{K_F} = (2500 + 239.42) \times 0.000434 = 1.19$ *in* [1.191*in*]

Eq.(23) gives; $\delta_C = \dfrac{1.191}{2} + \dfrac{500 \times 10^3 \times 12^3}{48 \times 29000 \times 124242} - \dfrac{(500 - 2 \times 239.42) \times 10^3 \times 12^3}{32 \times 29000 \times 124242} = 1.067$ *in* [1.06*in*]

Eq. (30) gives; $\omega = \dfrac{1}{2\pi}\left[\dfrac{(2500 \times 1.19 + 500 \times 1.06) \times 12}{(2500 \times 1.4161 + 500 \times 1.1236)}\right]^{\frac{1}{2}} = 0.51$ *hertz.* [0.51]

5. DEVELOPMENT OF RIGID ROCKING CORES

While the core is assumed to be rigid, its appendages are allowed to exhibit elastic-plastic behavior. Following Eq. (26) the roof level lateral displacement of the subject model in terms of drift ϕ, the frame and core spring stiffnesses K_F and K_S, can be expressed as;

$$\delta_F = \varphi h = \frac{M_0}{[h(K_F + K_S) - P]} = \frac{M_0}{\bar{K}_F} \tag{26}$$

where $M_0 = +(V_F + V_C)h/2$ and $P = W_f + W_m + W_c$. The disposition of the interactive forces between the frames and the core is presented in Figs. 5 (e) and (f). The lateral displacement of the rocking core composed of a rigid body displacement $\delta_F / 2$ and core bending δ_F can be estimated as;

$$\delta_C = \frac{\delta_F}{2} + \frac{V_C}{K_C} = \frac{\phi h}{2} + \frac{V_C}{K_C} \tag{27}$$

$$\delta_F = \phi h = \frac{(V_F + V_C)h}{2[h(K_F + K_S) - P]} = \frac{(1+\alpha_m)V_C h}{2\bar{K}_F} \tag{28}$$

$$\delta_C = \left[\frac{(1+\alpha_m)h}{4} + \beta_k\right]\frac{V_C}{\bar{K}_F} \tag{29}$$

where the ratio $\beta_k = \bar{K}_F / K_C$ describes a measure of the relative rigidity of the combined structure with respect to the flexural rigidity of the core acting as an upright simply supported beam or braced frame. In the absence of K_S and P or, $K_S = P/h$, β_k becomes $\beta_k = D_F / 2(1+\rho)D_{C.}$ Eqs. (28) and (29) are employed to develop the natural frequency equation of the subject system described below.

Example 2: Given the same data as for example 1, verify the validity of Eq. (26).

Solution: $\delta_F = \frac{(2500\times 10 + 500\times 5)\times 12}{[10(2304.147 + 4.167) - 0]} = \frac{330000}{120\times 2308.314} = 1.191in$ [same as example 1].

6. DYNAMICS – THE FREQUENCY EQUATION

Rayleigh's method of frequency analysis is ideally suited for the purposes of the current study [37]. It provides great insight into the dynamic behavior of two degree of freedom systems under combined gravity and lateral forces, such as the lean–to, rocking-core and moment-frame configuration depicted in Figs. 1 and 5. Rayleigh's method depends on the availability of deformation profiles that closely resemble the position of the structure at maximum amplitude for the fundamental mode of natural vibrations. Ideally the selected shape is expected to be related to a state of static equilibrium that is compatible with all boundary conditions. One such shape may be envisaged by assuming $V_F = W_F = W_f + W_m$ and $V_C = W_C$ corresponding to lateral displacements δ_F and δ_C, in which case the natural cycles per second (*hertz*) can be estimated as;

$$\omega = \frac{1}{2\pi}\left[\frac{g(W_F\delta_F + 2W_C\delta_C)}{W_F\delta_F^2 + 2W_C\delta_C^2}\right]^{\frac{1}{2}} = \frac{1}{2\pi}\left[\frac{g(\alpha_m\delta_F + 2\delta_C)}{\alpha_m\delta_F^2 + 2\delta_C^2}\right]^{\frac{1}{2}} \tag{30}$$

where g=32.2ft/sec^2 is the gravitational acceleration.

6.1 Preliminary design data

In general, seismic analyses begin with estimation of the first natural frequency of the structure under consideration. The challenge for the preliminary design of RRCERFs is the reliable estimation of the rigidity of a core such that would impose SDOF response on the combined system. It may be seen from Fig. 5 and Eq. (22) that as the core rigidity D_C tends towards infinity, the corresponding displacement δ_C tends towards half the maximum

displacement of the frame, i.e., $\delta_C \to \delta_F/2$. ASCE/SEI [38] requires the stiffness of the frame to be sufficient to control the drift of the structure at each story within the limits specified by the building code. If the net drift limit is indicated by $\phi_{all.}$, then the controlling system displacements would be equal to $\delta_F = \phi_{f,all.}h$ and $\delta_C = \phi_{c,all.}h/2$. The required rigidity D_F and D_C can now be estimated by substituting the controlled value of δ_F into the governing Eq. (11) or its expanded forms, Eq. (25). The net drift of the core can now be estimated as $\phi_{c,net} = (2\delta_C - \delta_F)/2h$. Since Eq. (15), implies a satisfactory degree of rigidity for the core then substitution of the δ_F and δ_C into Eq. (30) would result directly in the design first natural frequency;

$$\omega = \frac{1}{2\pi}\left[\frac{2g(1+\alpha_m)}{(1+2\alpha_m)\phi_{allow.}h}\right]^{\frac{1}{2}} \tag{31}$$

Two limiting conditions come to mind, 1- $\alpha_m \to \infty$, e.g., a highly rigid but lightweight core such an upright steel braced frame, Fig. 2(d), in which case $\omega^2 = g/4\pi^2\phi_{all.}h$, and 2- $\alpha_m \to 0$ a highly rigid but heavy weight core such as a reinforced concrete rocking wall, Fig. 2(c), in which case $\omega^2 = g/2\pi^2\phi_{all.}h$. A simple plot of variations of ω against α_m is presented in Fig.9, where it may be observed that the difference between the two extreme frequencies is $1/\sqrt{2}$ or about %30, and that in the practical range of variations, $\infty > \alpha_m > 0$, the natural frequency is insensitive to minor variations in the mass of the RRC. Eq. (10) can now be utilized in conjunction with Eq. (31) to determine the fundamental period of vibration of the RRCERF for any combination of ratios α_m, D_F/D_C and K_S/D_C, this process is illustrated best by numerical examples 3 and 4 below.

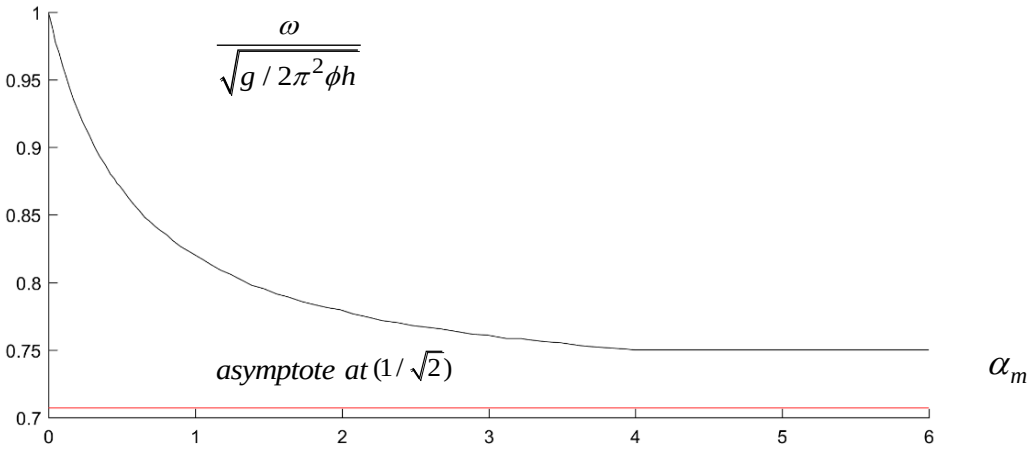

Figure 8. Variations of the system frequency (cps) with variations in RRC mass

Example 3: Infinitely stiff rocking core- determination of δ_F, δ_C and ω.

Solution: What happens if $D_C = \infty$? Evidently as $1/K_C \to 0$, $1/\overline{K}_C \to 0$ and $\delta_C = \delta_F / 2$

$$\alpha_m = \frac{500}{5000} = 0.1,\ \frac{1}{K_F} = 0.000434,\ \frac{1}{2K_S} = 0.12,\ \frac{1}{K_C} = 0.,\ \frac{1}{\overline{K}_C} = 0,\ \frac{1}{K_S} = \frac{144\times100}{5000\times12} = 0.24,$$

Eq. (22) gives; $Q = \dfrac{500\times0.12000 - 2500\times0.00044}{0.24043} = 245.0$ kips [245.07]

Eq. (12) gives; $\delta_F = \dfrac{V_f + Q}{K_F} = (2500 + 245.0)\times0.000434 = 1.191\ in$ [1.194*in*]

Eq. (25) gives; $\delta_C = \dfrac{\delta_F}{2} = \dfrac{1.192}{2} = 0.596$[0.597*in*]

Eq. (30) gives; $\omega = \dfrac{1}{2\pi}\left[\dfrac{(2500\times1.191 + 500\times0.596)\times12}{(2500\times1.4185 + 500\times0.3552)}\right]^{\frac{1}{2}} = 0.513 hertz.$ [0.517]

It may be noted that ω is practically the same for both the relatively stiff, Example 1, and infinitely rigid, Example 3 cores. In conclusion, even moderately stiff rocking cores stabilized by relatively stiff rotational (base level) springs can improve the lateral response of the system by as much as that associated with infinitely RRCs. The remainder of this article is concerned with establishing minimum core rigidities in terms of relative variables α_m, D_C / D_F and K_S / D_C.

Example4: Determine the minimum rigidities of the frame and the core for $\phi = 0.04$ radians, *E*=3500ksi, h=L=10.0ft., $V_f = 5000$ kips, $V_c = 500$ kips, $K_S = P = 0$, $\rho = 1.0$.

Solution: $\delta_F = \phi_{f,all.} h = 0.04\times10\times12 = 4.8in$, From Eq. (13) $Q = V_c/2 = 250$ kips. Eq. (14) gives $\phi_{f,all.} h = \dfrac{(V_f + V_c/2)h^3}{12D_F} \to D_F = \dfrac{(2500 + 250)\times10^2\times12^2}{12\times0.04} = 82.5\times10^6$ kip.in^2

$$\frac{\phi_{c,all} h}{2} = \frac{500\times10^3\times12^3}{48D_C} - \frac{(500 - 2\times250)\times10^3\times12^3}{32D_C} = 1.2 \to D_C = \frac{500\times10^3\times12^3}{48\times1.2} = 15\times10^6 \text{ kip.in}^2$$

7. CONCLUSIONS

It has been shown that earthquake resisting rocking core-moment frame combinations can be categorized as resilient provided that the rocking core is designed not to fail at maximum considered earthquake. It has also been argued that since the high rigidity of the core suppresses higher modes of vibrations the structure behaves as a single degree of freedom system, a fact that makes the proposed configuration eligible for linear and nonlinear static analysis. The design approach reported in this paper is different to conventional performance-based philosophies in that instead of looking at severity of damage, attention is focused on the ability of the rocking core and its appendages to prevent plastic collapse, to

realign and prepare the system for post-earthquake repairs.

In conclusion the following simple steps can be used to arrive at a preliminary design for a relatively rigid rocking core as part of a resilient earthquake resistant system.

1) Establish ϕ_{allow} in accordance with the requirements of the prevailing codes of practice,
2) Use Eq. (31) in to estimate the natural period of vibrations of the system and the seismic loading,
3) Utilize Eq. (13) and/or (25) to estimate K_F, K_s
4) Use Eq. (19) to compute the minimum strength of the un-supplemented rocking core,
5) Use rule 2.1 to estimate the minimum stiffness of the un-supplemented rocking core.

The paper suggests that the most important structural attributes of properly designed RRCs can be summarized as;

1) If the RRC is rigid enough the RRCERF can be regarded as a SDOF structure.
2) The zero line of reference passes through both ends of the RRC.
3) Imposition of uniform drift by the RRC prevents inactive hinges from engaging in plastic rotations.
4) RRCs exert the same internal distribution of forces on the frames as the external forces to the system, plus a roof level single force that acts in the same sense as the external loading.
5) RRC attached supplementary devices can improve the performance of the combined structure.
6) An RRC without auxiliary devices, can improve the drift but not the ultimate strength of the ERF.
7) RRCs can help prevent damage concentration within the members of the primary structure.
8) RRC forces points of inflection of the MF to move towards mid-spans of all beams and columns.
9) Residual drifts significantly contribute to the overall earthquake loss.
10) Residual drifts impact if buildings are safe for occupancy after an earthquake.
11) The drift angle can be used to control the performance of the RCERFs under lateral loading.
12) The normalized drift function remains unchanged throughout the loading history of the structure.
13) Loss of stiffness changes only the value of the drift angle but not the drift profile.
14) The drift profile is a function of the same single variable for all loading conditions.
15) The uniform drift of a RRCERF is given by the total overturning moment divided by the global rotational stiffness of the system.
16) Even the first approximation for core stiffness results in practically acceptable dimensions.
17) The degree of effectiveness of RRCERFs, with or without supplementary devices, should be carefully examined for new as well as retrofit projects.
18) A poorly performing free-standing ERF can be turned into a highly efficient RRCERF.
19) RRCERFs are ideally suited for implementing CP and PERR technologies.
20) Supplementary devices such as stressed tendons can be used effectively to increase the equivalent stiffness of the RRCERF combinations.
21) The addition of the base level attachments can considerably improve the drift as well as the carrying capacity of the system.
22) The dominant mode shapes remain unchanged during all phases of loading.
23) The structure is an SDOF system, and as such, lends itself well to equivalent energy studies.
24) RRCs can prevent ERF collapse due to formation of plastic failure mechanisms.

Other important attributes drawn from companion research has been summarized in Appendix B below.

APPENDIX A: TRADITIONAL METHOD OF SIZING OF RRCS

It has been observed that regardless of type of the earthquake resisting system, whether an eccentrically braced frame, MF or any other reliable configuration, the RRC performs best when its stiffness approaches infinity, However, experience has shown that for high levels of RRC to frame rigidity ratios the maximum uniform drift is not sensitive to minor variations in the relative rigidities of the two systems. In other words, for practical design purposes the stiffness of the RRC can be related to a fraction of the code prescribed uniform drift ϕ of the combined system, say $\varepsilon\%\varphi$ or $\psi_{\max} = \bar{\varepsilon}\varphi$. The following design data may be found useful for the preliminary estimation of rigidities of RRC under uniform (A1), and triangular (A2), distributions of lateral forces;

$$\psi_{max} = \frac{Fh^2 m(m-1)(m^2+m-2)}{24E_w I_w} \;\&\; I_{w,\min} = \frac{Fh^2(m-1)(m^2+m-2)}{24E_w\bar{\varepsilon}\phi} \tag{A1}$$

$$\psi_{\max} = \frac{Fh^2(m-1)(2m-1)(2m^2+3m-4)}{180E_w I_w m} \;\&\; I_{w,\min} = \frac{Fh^2(m-1)(2m-1)(2m^2+3m-4)}{180E_w\bar{\varepsilon}\phi m} \tag{A2}$$

APPENDIX B: ADDITIONAL STRUCTURAL ATTRIBUTES OF PROPERLY DESIGNED RRCS FROM COMPANION RESEARCH [3, 9, 13 &17] CAN BE SUMMARIZED AS;

1) RRCs are capable of helping eliminate residual drifts and limiting damage to replaceable fuses.
2) The RRC acts as an upright simply supported beam subjected to self-equilibrating forces.
3) Regardless of the properties of the RRC, it can have no effect on the static performance of SUR.
4) The RRC forces the moment frame to act as a SUR.
5) A highly rigid but not infinitely stiff RRC can be used to achieve performance control.
6) RRC supported MFUS have the same ultimate strength as their equivalent free standing MFUR.
7) The properties of the RRC have no effect on the plastic displacements of well-proportioned MFs.
8) An ERF supported by a RRC is as efficient as its optimized free-standing counterpart.
9) Pin supported RRCs reduce the seismic moment demand on their footings.
10) The RRC can be effective if the drift profile of the ERF contains appreciable drift differentials.

11) Regular, uniform stiffness wall-frames can be construed as structures of minimum weight.
12) RRCERFs with supplementary devices are ideally suited for all performance level applications.
13) RRCERFs designs using linear elastic–plastic procedures pass the test of time-history analysis.
14) RRCERFs deform the same way as free-standing SUR.
15) RRCERFs response can be improved considerably by selecting the properties of certain groups of elements in accordance with design led strategies.
16) Extensive static and dynamic computer analysis support the viability of the proposed solutions.

REFERENCES

1. Wada A, Qu Z, Ito H, Motoyui S, Sakata H, Kasai K. Pin supported walls for enhancing the seismic behavior of building structures, *Earthq Eng Struct Dyn* 2012; **41**(14): 2075-91.
2. Deierlein GG, Ma X, Eatherton M, Hajjar J, Krawinkler H, Takeuchi T. Collaborative research on development of innovative steel braced frame systems with controlled rocking and replaceable fuses, *Proceedings of the 6th International Conference on Urban Earthquake Engineering*, Tokyo, 2009; 413-6.
3. Grigorian C, Grigorian M, Performance control and efficient design of rocking-wall moment-frames, *J Struct Div ASCE* 2015a, DOI: 10.1061/ (ASCE) ST.1943-541X.0001411.
4. Stevenson M, Panian L, KorolyK M, Mar D. Post-Tensioned Concrete Walls and Frames for Seismic-Resistance - A Case Study of the David Brower Center, *Seaoc 2008 Convention Proceedings*; 1-8.
5. Janhunen B, Tipping S, Wolfe J, Mar D. Seismic retrofit of a 1960s steel moment- frame high-rise using a pivoting spine, *Proceedings of the Annual Meeting of the Los Angeles Tall Buildings Structural Design Council*, Los Angele, 2012.
6. Pollino M, Slovenec D, Qu DS, Mosqueda G. Seismic rehabilitation of concentrically braced frames using stiff rocking core, *J Struct Eng* 2017; 143(9).
7. Hajjar JF, Sesen AHT, Jampole E, Wetherbee A. A synopsis of resilient structural systems with rocking, self-centering and articulated energy-dissipating fuses, Rep. No. NEU-CEE-2013-01, Department of Civil and Environmental Engineering Reports, Northeastern University, Boston.
8. Eatherton MR, Ma X, Krawinkler H, Mar D, Billington S, Hajjar JF, Deierlein GG. Design concepts for controlled rocking of self-centering steel-braced frames, *J Struct Eng* 2014; 10.1061/(ASCE)ST.1943-541X.0001047.
9. Grigorian M, Grigorian C. An Introduction to the structural design of rocking wall - frames with a view to collapse prevention, self - alignment and repairability, *Struct Des Tall Special Build* 2015b; DOI: 101002/tal.1230.
10. Elsesser E. Seismically resistant design – past, Present, Future, *13th World Conference on Earthquake Engineering*, Paper No. 2034, Vancouver, B.C., Canada, 2004.

11. Chancellor NB, Eatherton MR, Roke DA, Akbas T. Self-centering seismic force resisting systems: High performance structures for the city of tomorrow, *Build* 2014; **4**: 520-48,
12. Shen Y, Christopoulos C, Mansour N, Tremblay R. Seismic design and performance of steel moment-resisting frames with nonlinear replaceable links, *J Struct Eng* 2011; **137**(10): 1107-17.
13. Grigorian M, Grigorian C. Resilient earthquake -resisting system, *J Struct Div ASCE* 2018, DOI: 10.1061/(ASCE)ST.1943-541X.0001900.
14. Pessiki S. Resilient seismic design, *Proced Eng* 2017; **171**: 33-9.
15. Cimellaro GP. New trends on resiliency research, *16th World Conference on Earthquake Engineering* 2017; 16WCEE, Chile.
16. Qu B, Sanchez J, Hou H, Pollino M. Improving inter-story drift distribution of steel moment resisting frames through stiff rocking cores, *International Journal of Steel Structures* 2016; **16**(2): 547-57.
17. Qu B, Sanchez-Zamora F, Pollino M. Transforming seismic performance of deficient steel concentrically braced frames through implementation of rocking cores, *ASCE J Struct Eng* 2015; **141**(5).
18. Qu B, Sanchez-Zamora F, Pollino M. Mitigation of inter-story drift concentration in multi-story steel concentrically braced frames through implementation of rocking cores, *Eng Struct* 2014; **70**: 208-17.
19. Qu B, Guo X, Chi H, Pollino M. Probabilistic evaluation of effect of column stiffness on seismic performance of steel plate shear walls, *Eng Struct* 2012; **43**:169-79.
20. Roke DA, Hasan MR. The effect of frame geometry on the seismic response of self-centering concentrically-braced frames, *Int J Civil Environ Eng* 2012; **6**: 140-5.
21. ASCE/SEI 2014 Sustainability Committee, http://www.asce.org/sustainability/.
22. Grigorian, M., Moghadam, A.S., Mohammadi, H. and Kamizi, M., 2019. Methodology for developing earthquake resilient structures. *The Structural Design of Tall and Special Buildings*, *28*(2), p.e1571. https://doi.org/10.1002/tal.1571.
23. Grigorian M, Moghadam AS, Mohammadi H. Advances in rocking-core moment frame analysis, *Bullet Earthq Eng* 2017b; **15**(12): 5551-77.
24. Grigorian C, Popov E, Yang T. Developments in seismic structural analysis and design, *Eng Struct* 1995; **17**(3): 187-97.
25. Taylor Devices, www.taylordevices.com.
26. Grigorian M, Grigorian C. Performance control: A new elastic-plastic design procedure for earthquake resisting moment frames, *J Struct Div* 2012a; **138**(6).
27. Grigorian M, Grigorian C, Recent developments in plastic design analysis of steel moment frames, *J Construct Steel Res* 2012b, 7683–92.
28. MacRae GA, Kimura Y, Roeder C. Effect of column stiffness on braced frame seismic behavior, *J Struct Div* 2004; 1**30**(3): 381-91.
29. Seymour D, Laflamme S. Quasi-Static analysis of rocking wall systems, Department of civil and environmental engineering, Massachusetts Institute of Technology, Cambridge, http://works.bepress.com/simon_laflamme/5.
30. Wiebe L, C. Christopoulos C. Mitigation of higher mode effects in base-rocking systems by using multiple rocking sections, *J Earthq Eng* 2009; **13**(S1): 83-108.

31. Aalavi B, Krawinkler H. Behaviour of moment-resisting frame structures subjected to near-fault ground motions, *Earthq Eng Struct Dyn* 2004; **33**(6): 687-706.
32. Garlock M, Sause R, Ricles J. Behavior and design of post-tensioned steel frame systems, *J Struct Eng ASCE* 2007; **133**(3): 389-99.
33. Dowden DM, Bruneau M. New Z-BREAKSS: Post-tensioned rocking connection detail free of beam growth, *AISC Eng J* 2011; 2nd, Quart 153-158.
34. Taranath BS. *Steel, Concrete and Composite Design of Tall Buildings*, 2nd ed, Mc GrawHill, 1998.
35. Mazzolani M. Plastic design of seismic resistant steel frames, *Earthq Eng Struct Dyn* 1997; **26**(2): 167-9.
36. Grigorian M, Grigorian C. Lateral displacements of moment frames at incipient collapse, *Eng Struct* 2012c; 174-85.
37. Grigorian M. On the dynamic analysis of regular shear structures, *Earthq Spectra* 1993; **9**(1): 55-65.
38. ASCE/SEI 7-10. *Minimum Design loads for Buildings and Other Structures*, ASCE/SEI Standard 7-10, American Society of Civil Engineers, Reston, VA., US, 2010.